

EFFECTS OF TEMPERATURE ON THE STRUCTURAL AND OPTICAL PROPERTIES OF AgGaSe₂ THIN FILMS

M.R.A. BHUIYAN*, D.K. SAHA¹ AND S.M. FIROZ HASAN²

Department of Applied Physics, Electronics and Communication Engineering, Islamic University, Kushtia-7003, Bangladesh

(Received revised copy: August 2, 2009)

ABSTRACT

In this study, AgGaSe₂ (AGS) thin films were formed onto cleaned glass substrates by using the stacked elemental layer (SEL) deposition technique in vacuum. The films were prepared at the post-deposition annealing temperature from 100 to 350°C for 15 min duration. The atomic composition of the films was measured by energy dispersive analysis of X-ray (EDAX) method. The films ascertain the compositional uniformity. The X-ray diffraction (XRD) has been employed to study the structure of the films. The structures of the films are found to be polycrystalline in nature. The lattice parameters, grain size, strain and dislocation densities of the films were calculated. Optical characteristics of the films were ascertained by spectrophotometer in the photon wavelength ranging between 300 and 2500 nm. The transmittance was found to increase with the increase of annealing temperature. The transmittance falls steeply with decreasing wavelength. It revealed that AGS films have considerable absorption throughout the wavelength region from 400 to 800 nm. The optical band gap energy has been evaluated. Two possible direct allowed and direct forbidden transitions have been observed for all the AGS films in visible region. The former varied from 1.67 to 1.75 eV and the later from 2.05 to 2.08 eV, depending on the post-deposition annealing temperature of the films.

INTRODUCTION

In recent years, there has been a great deal of interest in the study of ternary semiconducting materials as well as technological point of views. This semiconductor appears to be a promising element for thin film solar cells due to its near-optimum band gap energy, high optical absorption coefficients and long-term-stability.⁽¹⁾ AGS belongs to the group of I-III-VI₂ semiconducting materials with tetrahedral coordinates and crystallizes with a tetragonal chalcopyrite structure.⁽²⁾ It is known that chalcopyrite compound semiconductors are direct band gap materials, showing a two optical structure near the fundamental edge due to crystal-field and spin-orbit splitting of the uppermost valence band. Studies on AGS thin films as absorber material are still more attractive, since they allow tailoring of the optical band gap and other properties. Silver indium selenide (AIS), the most prospective thin-film material obtained so far for photovoltaic applications, has been extensively studied.⁽³⁻⁵⁾ One of the problems with AIS is that its band gap energy is somewhat low to match the optimum solar spectrum. Substituting indium by gallium in

* Corresponding author: E-mail: mrab_ju@yahoo.com (MRA Bhuiyan)

¹ Materials Science Division, Atomic Energy Centre, GPO Box 164, Dhaka-1000, Bangladesh

² Experimental Physics Division, Atomic Energy Centre, GPO Box 164, Dhaka-1000, Bangladesh

AgInSe₂, the optical band gap can be increased from 1.25 to 1.75 eV.⁽⁶⁾ AGS is minimal⁽⁷⁻¹⁰⁾ as far as the thin film form is concerned. It has been proved to be stable and efficient absorber materials for fabricating polycrystalline thin film heterojunction solar cells.^(11, 12) A better understanding of the structural and optical properties is essential for optimizing these films for solar cell fabrication. Hence, an attempt has been made to study the post-deposition annealing temperature effects on the structural and optical properties of AGS thin films.

EXPERIMENTAL

Growth of the films

The films of silver, gallium and selenium were deposited sequentially onto chemically and ultrasonically cleaned glass substrates by thermal evaporation of individual elemental layers to form a stack, in vacuum ($\approx 10^{-7}$ mbar) by using oil diffusion pump (E306A, Edwards, UK). The thickness of the stoichiometric films was 500 ± 50 nm. In our previous report,⁽¹³⁾ we described the growth of AGS thin films.

Compositional measurements

The elemental atomic composition of the samples was accomplished with an energy dispersive analysis of X-ray (EDAX) attachment with the scanning electron microscope (SEM) (Philips XL-30 system).

Structural measurements

The X-ray diffraction (XRD) was used to investigate the structure of AGS thin films. The diffraction patterns were recorded using a Philips PW 3040 X'Pert PRO XRD system with Cu-K α radiation, operated at 40 KV and 30 mA, with angular range $20^\circ \leq 2\theta \leq 50^\circ$.

Optical measurements

The variations of transmittance and specular absolute reflectance of the films with wavelength of light incident on them were measured by using a dual beam UV-VIS-NIR recording spectrophotometer (Shimadzu, UV-3100, Japan) in the photon wavelength ranging between 300 and 2500 nm. We have employed these measurements in our previous reports.^(14, 15)

RESULTS AND DISCUSSION

Compositions at three different places on each sample were determined by energy dispersive analysis of X-ray (EDAX) method. They show reasonably identical values (± 0.01 at.%) that ascertain the compositional uniformity of the sample. In our previous report,⁽¹⁴⁾ we addressed the typical EDAX spectrum of AgGaSe₂ thin film having stoichiometric. In our observation, all films are found to be stoichiometric with different annealing temperatures.

Fig. 1 shows the X-ray diffraction patterns of stoichiometric AGS films having different temperatures. The X-ray diffraction revealed that the films were polycrystalline in nature. Expected peak^(16, 17) for AGS thin films are (112), (201), (211), (220), (204), (301) and (312). But in our films (110), (112), (211), (114), (220), (204) and (310) peaks are present. The intensity and position of (112) peak is in good agreement with ASTM data for tetragonal silver gallium selenide. The (112) peak is prominent peak for AGS thin films. Other workers obtained (112) peak of higher intensity.^(16, 17) In our case, the films annealed at 200, 250 and 350°C show low-intensity (112) peak. This peak is absent for the film annealed at 100°C. Sample annealed at 300°C shows (112) peak of higher intensity. The high intensity of reflection from the (112) plane indicates the preferred orientation.⁽¹⁸⁾

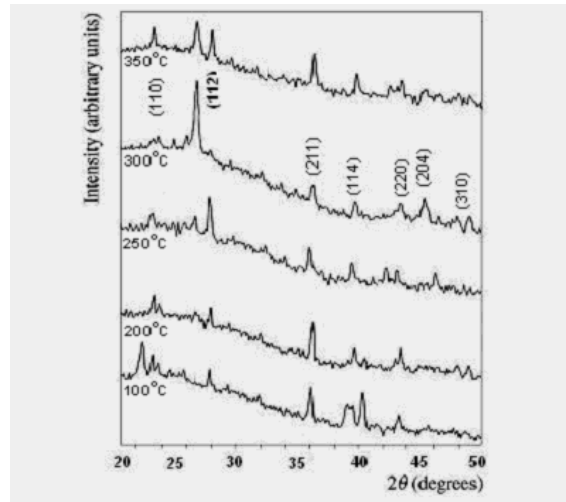


Fig. 1. The XRD spectra of AGS thin films having different temperatures of deposition.

In our previous report,⁽¹⁵⁾ we addressed the variation of lattice parameters and grain size with different annealing temperatures. It exhibits tetragonal chalcopyrite structure with average lattice parameters, $a \approx 6.00 \text{ \AA}$ and $c \approx 10.92 \text{ \AA}$ and $c/a = 1.82$. A qualitative estimate of the grain size of the films deposited at different annealing temperature was calculated by using the well-known Scherrer's formula⁽¹⁹⁾ simplified by Bragg

$$B_{\text{crystallite}} = \frac{0.9\lambda}{B \cos \theta} \quad (1)$$

where λ is the wavelength of Cu K α radiation, and B is their full-width half-maximum (FWHM). The unit of B should be converted into radian. Therefore, the above equation takes the form,

$$B_{\text{crystallite}} = \frac{50.97 \lambda}{B \cos \theta} \quad (2)$$

The average grain size of the films was calculated to be 40 nm, which conforms reasonably well to the literature value.⁽¹⁶⁾ The lattice parameters are independent unlike

the grain size that varies directly with annealing temperatures. The grain size increases with increasing annealing temperature. When annealing temperature increases the line width becomes narrow due to the increase in grain size. Narrower peak also reflects the decrease in the concentration of lattice imperfection due to the decrease in the internal microstrain within the film.⁽²⁰⁾ Similar results have been reported by other workers.^(21, 22) Larger grain size minimizes the imperfect regions of the film, which is also supported by the smaller strain and dislocation densities.

The strain, ε was calculated by using the following formula⁽²³⁾

$$\varepsilon = \frac{B \cos \theta}{4} \quad (3)$$

The dislocation density, δ defined as the length of dislocation lines per unit volume of the crystal, was evacuated from the formula⁽²³⁾

$$\delta = \frac{1}{(B_{\text{crystallite}})^2} \quad (4)$$

Strain and dislocation densities decrease as annealing temperature increases (Fig. 2). Since dislocation density and strain are the manifestation of dislocation network in the films, the decrease in dislocation density indicates the formation of high-quality films.⁽²⁴⁾ The inhomogeneous strain component is localized at the sub grain and sub domain level near grain boundaries. Pertsev and Arlt⁽²⁵⁾ introduced a fictitious dislocation density to model the inhomogeneous strain. The spontaneous strain in their model is analogous to the mechanical plastic deformation, for instance, in metals. This facilitates the analysis substantially because models developed for dislocations can be readily applied. They obtained two components of strain/stress fields: a homogeneous volume component extending over the whole grain volume and an inhomogeneous component concentrated near grain boundaries. We argue that dislocation effects are a real origin of inhomogeneous strains in AgGaSe₂ thin films and that large changes in dislocation density and configuration may occur. This is possibly because of the fact that when the annealing temperature is kept at 300°C, the dislocations get more thermal energy. These are the manifestation of dislocation network in the films. The decrease indicates the formation of high-quality films at higher annealing temperatures.⁽²⁶⁾ The structural parameters are shown in Table 1.

Table 1.
The structural parameters of AGS thin film having different annealing temperatures.

Annealing Temperature, T _A (°C)	Lattice Parameters		Grain size (nm)	Strain, $\varepsilon \times 10^{-4}$ (line ⁻² m ⁻⁴)	Dislocation density, $\delta \times 10^{14}$ (line/m ²)
	a (Å)	c (Å)			
100	5.93	11.32	14.85	23.20	45.34
200	6.00	10.91	17.10	20.13	34.20
250	5.99	10.89	34.20	10.11	8.64
300	6.01	10.93	41.04	8.38	5.93
350	5.99	10.89	45.90	7.50	4.74

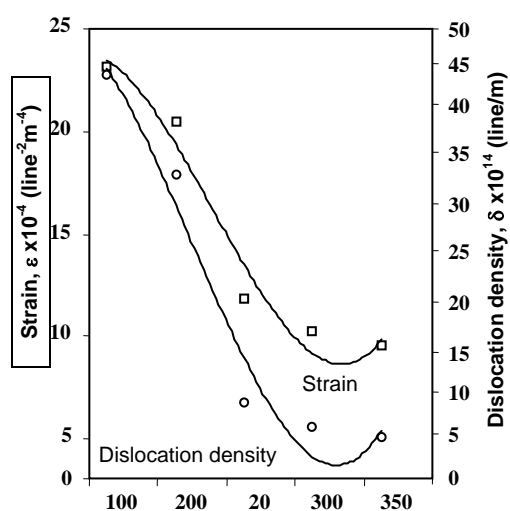


Fig. 2. Dependence of strain and dislocation density of AGS thin films having different temperatures.

Fig. 3 shows the optical transmittance and reflectance spectra of five films that are annealed for 15 min at different temperatures from 100 to 350°C. From the transmittance pattern it is clear that the ternary compound of AGS is not formed at the annealing temperature of 100°C as the corresponding spectrum does not show any well-defined absorption region.

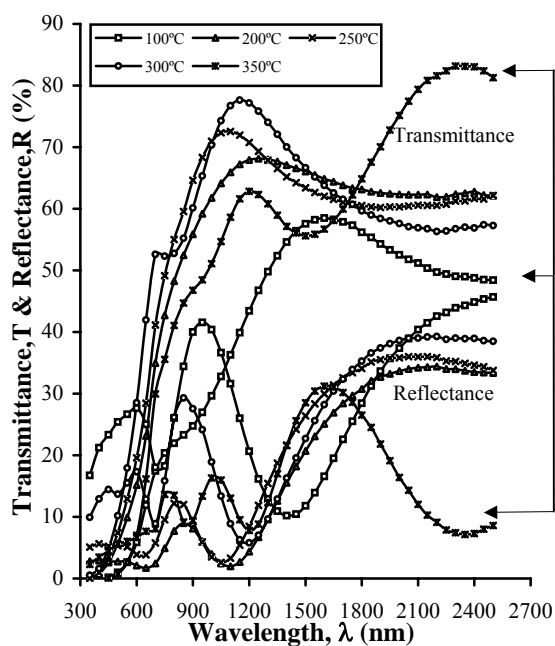


Fig. 3. Dependence of optical transmittance and reflectance on photon wavelength for AGS thin films having different temperatures.

If the sample is annealed at 200°C for 15 min, it goes to attain semiconducting properties, which indicates adherence to the formation of compound starting at this temperature. The transmittance spectrum attains its perfect shape for the sample annealed at 300°C for 15 min. Same inference can be drawn from the reflectance curves. The film annealed at 300°C for 15 min is better than that annealed at other temperatures. The better quality of the material annealed at 300°C for 15 min has also been ascertained from absorption coefficient spectra as shown in our previous report.⁽¹⁵⁾

In our previous report,⁽¹⁵⁾ we addressed the absorption coefficient curve of the film annealed at 300°C for 15 min has lower sub-band gap absorption and steeper fundamental absorption region. Most of the films show tail absorptions. This tail absorption occurs due to departure of the lattice structure from perfect periodicity. This departure is caused owing to the presence of thermal lattice vibrations and lattice imperfections and/or trapping sites located in the grain boundaries in particular. Absorption of optical energy can occur in the scattering process. Scattering broadens the absorption threshold. Generally, the broadening or shift is dominated by transitions involving optical phonon absorption.⁽²⁷⁾ Tell *et al*⁽²⁸⁾ have also found shallow defects or impurities in bulk AGS. In our observation, the optical absorption behavior of the films above the fundamental absorption edge can be interpreted by considering the existence of two types of optical transitions. The nature of the first transition (band gap) is direct allowed and the subsequent one is direct forbidden. Analysis of the absorption coefficient, α above the fundamental edge that it has high values ($\sim 10^5 \text{ cm}^{-1}$) and the rise of α in the photon energy range $1.773 \leq h\nu \leq 2.068 \text{ eV}$ follows a relation for an allowed direct interband transition,⁽²⁹⁾ described by

$$\alpha = \frac{A_1}{h\nu} \left[h\nu - E_{g1} \right]^{1/2} \quad (5)$$

where, E_{g1} is the band gap energy of the interband transition and A_1 is a parameter that depends on the probability of transition and the refractive index of the material. The transition energy E_{g1} , and the value of A_1 were found out from the plot of $(\alpha h\nu)^2$ versus $h\nu$ in the range $1.773 \leq h\nu \leq 2.068 \text{ eV}$. Direct allowed transitions vary between 1.67 and 1.75 eV depicted in Fig. 4.

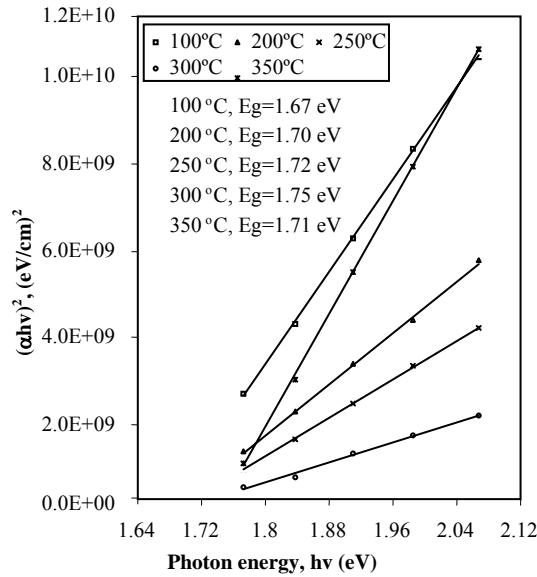


Fig. 4. Variation of $(\alpha hv)^2$ vs photon energy extracted from absorption coefficient.

Now, if we calculate the absorption coefficient for $h\nu > 2.068$ eV putting the obtained values of E_{g1} and A_1 , in equation (5) and call it α_1 (theoretical α) then we find that α_1 is smaller than the experimentally measured absorption coefficient, α . This discrepancy can only be explained by assuming an additional absorption $\alpha_2 = \alpha - \alpha_1$ above 2.068 eV of photon energy. The additional absorption curve, (α_2) is further analyzed and found that it follows the relation for direct forbidden interband transition quite well for $2.25 \leq h\nu \leq 2.75$ eV described by

$$\alpha_2 = \frac{A_2}{h\nu} [h\nu - E_{g2}]^{3/2} \quad (6)$$

The so-called forbidden energy gap E_{g2} and the parameter A_2 were extracted from the plot of $(\alpha_2 h\nu)^{2/3}$ versus $h\nu$, as shown in Fig. 5. The optical parameters are shown in Table 2.

Table 2.
The optical parameters of AGS thin film having different annealing temperatures.

Annealing temperature (°C)	E_{g1} (eV)	A_1 ($\text{cm}^{-1} \text{eV}^{1/2}$)	E_{g2} (eV)	A_2 ($\text{cm}^{-1} \text{eV}^{-1/2}$)
100	1.67	1.554E+05	2.07	2.813E+05
200	1.70	1.246E+05	2.08	1.247E+05
250	1.72	1.077E+05	2.06	1.173E+05
300	1.75	7.814E+04	2.08	1.349E+05
350	1.71	1.422E+05	2.05	1.533E+05

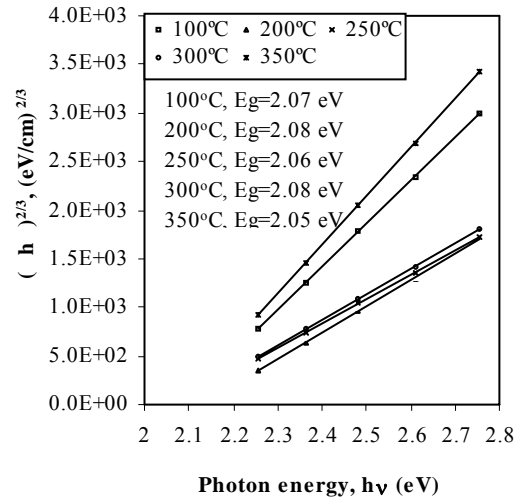


Fig. 5. Variation of $(\alpha h\nu)^{2/3}$ vs photon energy extracted from absorption coefficient.

Direct allowed transition increases as annealing temperature increases and attains its maximum value of 1.75 eV at 300°C (conforming to the literature value). The direct allowed transition decreases for further increase of annealing temperature. This indicates that at the post-deposition annealing temperature of 300°C, the material becomes perfect in structure. This prediction was also confirmed by the XRD studies. Direct forbidden transition has no such correlation with annealing temperature.

Fig. 6 shows the dependence of optical absorption coefficient on annealing temperature at wavelengths 1750 and 2450 nm. At the annealing temperature of 300°C, the films show minimum sub-band gap absorption. This also ascertains the preference of annealing temperature to be 300°C for attaining better quality of the films.

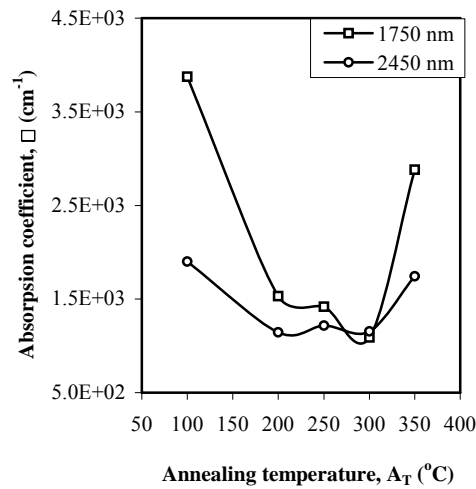


Fig. 6. Dependence of absorption coefficient on temperature for AGS thin films at wavelengths 1750 and 2450 nm.

CONCLUSIONS

The films were reasonably homogeneous in composition as evident from the EDAX data at various locations on the films. The XRD reveals that the films were polycrystalline in nature. The lattice parameters are independent unlike the grain size that varies directly with annealing temperatures. The strain and dislocation density vary indirectly with post-deposition annealing temperatures. The optical absorption behaviour of AGS thin films above the fundamental absorption edge can be interpreted by considering the existence of two types of optical transitions from valence band to conduction band. The first transition, E_{g1} is direct allowed and the subsequent one, E_{g2} is direct forbidden. The E_{g1} varies directly with the post-deposition annealing temperature while E_{g2} shows no such correlations. Hence, by the present investigation, we can grow the films of AGS having different energy gaps. This skill of varying energy gap of AGS may be worth fabricating device, such as thin film solar cell absorber.

ACKNOWLEDGEMENTS

The author (MRAB) is grateful to the University Grants Commission of Bangladesh for granting me a Ph.D. fellowship for carrying out this work. We are also thankful to Mr. Syed Ayubur Rahman, Ms. Jahanara Parvin for their assistance in preparing the samples.

REFERENCES

1. U. RAU AND H. W. SCHOCK, *Appl. Phys. A: Mater. Sci. Process*, **69**, 131, 1999.
2. J. L. SHAY AND J. H. WERNICK, *Ternary Chalcopyrite Semiconductors: Growth, Electronic Properties and Applications*, Pergamon Press, Oxford, 1975.
3. P. P. RAMESH, S. UTHANNA, B. S. NAIDU AND P. J. REDDY, *Thin Solid Films*, **292**, 290, 1997.
4. P. P. RAMESH, O. M. HUSSAIN, S. UTHANNA, B. S. NAIDU AND P. J. REDDY, *Mater. Sci. Eng.: B*, **49**, 27, 1997.
5. P. P. RAMESH, O. M. HUSSAIN, S. UTHANNA, B. S. NAIDU AND P. J. REDDY, *Mater. Lett.*, **34**, 217, 1998.
6. G. H. CHANDRA, O. M. HUSSAIN, S. UTHANNA AND B. S. NAIDU, *Vacuum*, **62**, 39, 2001.
7. S. M. PATEL AND V. G. KAPALE, *Mater. Lett.*, **3**, 440, 1985.
8. S. M. PATEL AND V. G. KAPALE, *Mater. Lett.*, **4**, 145, 1986.
9. Y. S. MURTHY, B. S. NAIDU AND P. J. REDDY, *Vacuum*, **41**, 1448, 1990.
10. Y. S. MURTHY, S. UTHANNA, B. S. NAIDU AND P. J. REDDY, *Solid State Comm.*, **79**, 287, 1991.
11. Y. S. MURTHY, O. M. HUSSAIN, B. S. NAIDU AND P. J. REDDY, *Mater. Lett.*, **10**, 504, 1991.
12. Y. S. MURTHY, B. S. NAIDU AND P. J. REDDY, *Mater. Sci. Eng.: B*, **8**, 175, 1991.
13. M. R. A. BHUIYAN AND S. M. FIROZ HASAN, *Sol. Energy Mater. Sol. Cells*, **91**, 148, 2007.
14. M. R. A. BHUIYAN AND S. M. FIROZ HASAN, *J. Phys. D: Appl. Phys.*, **39**, 4935, 2006.
15. M. R. A. BHUIYAN, M. K. RAHMAN AND S. M. FIROZ HASAN, *J. Phys. D: Appl. Phys.*, **41**, 235108, 2008.
16. H. S. SOLIMAN, *J. Phys. D: Appl. Phys.*, **28**, 764, 1995.
17. Y. S. MURTHY, O. M. HUSSAIN, B. S. NAIDU AND P. J. REDDY, *21 PVSC*, **1**, 487, 1990.
18. Y. D. TEMBHURKAR AND J. P. HIRDE, *Thin Solid Films*, **215**, 65, 1992.

19. C. S. BARETT, *Structure of Metals Crystallographic Methods Principles and Data*, McGraw-Hill, New York, 1956.
20. S.A. AL KUHAIMI, *Vacuum*, **51**, 349, 1998.
21. L. KERKACHE, A. LAYADI, E. DOGHECHE AND D. REMIENS, *J. Phys. D: Appl. Phys.*, **39**, 184, 2006.
22. P.S. RAGHUPATHI, J. GEORGE AND C. S. MENON, *Indian J. Pure Appl. Phys.*, **43**, 620, 2005.
23. S. LALITA, R. SATHYAMORTHY, S. SENTHILARASU, A. SUBBARAYAN AND K. NATARAJAN, *Sol. Energy Mater. Sol. Cells*, **82**, 187, 2004.
24. U. PAL, D. SAMANTHA, S. GHORAI S AND A. K. CHAUDHURI, *J. Appl. Phys.*, **74**, 6368, 1993.
25. N. A. PERTSEV AND G. ARLT, *Sov. Phys. Solid State*, **33**, 1738, 1991.
26. R. SATHYAMOORTHY, S. K. NARAYANDASS AND D. MANGALARAJ, *Sol. Energy Mater. Sol. Cells*, **76**, 339, 2003.
27. E. J. JOHNSON, *Semiconductors and Semimetals Academic Press*, New York, 1967.
28. B. TELL AND H. M. KASPER, *Phys. Rev. B*, **4**, 4455, 1971.
29. S. M. PATEL AND V. G. KAPALE, *Thin Solid Films*, **148**, 143, 1987.